PHYSICAL REVIEW B VOLUME 15, NUMBER 10 15 MAY 1977

Theory of indirect excitons in semiconductors

N. O. Lipari*
Xerox Webster Research Center, Xerox Corporation, Xerox Square-114, Rochester, New York 14644

M. Altarelli†
Department of Physics and Materials Research Laboratory, University of Illinois, Urbana, Illinois 61801
(Received 6 January 1977)

The effective-mass Hamiltonian for indirect excitons in cubic semiconductors is solved. The approach used allows a physical interpretation of the various terms in the Hamiltonian thus making possible the introduction of simpler but equally accurate models. In particular, the "axial model" is described, which is very suitable for the investigation of various problems. The validity of this model is discussed and shown to depend on the relative strength of the electron anisotropy and of the hole anisotropy. By using rotation-group techniques the angular and the radial part in the exciton Hamiltonian are separated and the problem is reduced to a system of radial differential equations. All the experimentally observed exciton levels are calculated. A comparison with the results obtained by the perturbative approach is given and analytical expressions for the most relevant exciton states are obtained in the perturbative limit. Recent experimental data for Ge are analyzed and excellent agreement with our calculations is obtained. Comparison is also made for Si and GaP. The usefulness of the present approach for the treatment of other problems is discussed.

I. INTRODUCTION

Excitons constitute the lowest electronic excited states of semiconductors and therefore play a fundamental role in their optical properties.[1] The discovery of the electron-hole condensation in indirect semiconductors[2] and the advances in modulation spectroscopy[3] have led to an increasing interest in the understanding of indirect excitons. The first observation of indirect excitons was made in Si and Ge.[4] Since then, structure due to exciton formation has been observed by many investigators.[5] Modulation spectroscopy at indirect edges has provided new and accurate data on exciton binding energies, and, very recently Frova *et al.*[3] have reported the first experimental observation of the "mass-reversal" effect, which is due to the strong nonparabolicity of the two 1*s* exciton bands in Ge, split by the anisotropy of the conduction-band minima. In addition, measurements in a region corresponding to the exciton binding energy, i.e., in the far-infrared region, have provided more detailed information on the structure of the excitons. After the first measurements which were performed by Gershezon *et al.*,[6] more accurate investigations have been performed by several investigators.[7-9] The most recent of these studies is that by Buchanan and Timusk.[10] These spectra reveal a wealth of resolved fine structure which has been attributed to transitions from the anisotropy split ground state to higher excited states of the exciton.

Excitons are usually visualized by the familiar analogy to the hydrogen atom. This picture is quantitatively accurate only for a model semiconductor with nondegenerate isotropic and parabolic valence and conduction bands. All crystals with the diamond and zinc-blende structure have a degenerate valence band at the center of the Brillouin zone.[11] In addition, the absolute minimum of the conduction band is sometimes at the same point of the Brillouin zone, while in other cases such minimum is at $K \neq 0$, and its location depends on the particular substance under consideration. For germanium,[12] the minimum is at the point $L = (\pi/a)(111)$ and[13] Si is along the $\Delta \equiv (K, 0, 0)$ direction. Other zinc-blende compounds such as AlP,[14] AlSb,[15] AlAs,[14] and GaP,[16] have also indirect gaps. For direct excitons, which have a parabolic and isotropic conduction band, the perturbative analysis, previously introduced by Baldereschi and Lipari,[17-19] describes accurately the excitonic spectrum, since the only anisotropy present is that in the valence band. Simple analytical expressions for the most important exciton states were obtained which are very useful in the interpretation of the experimental spectra. In contrast, for indirect excitons there is an additional strong anisotropy in the conduction-band masses. The ratio between masses in different directions is as high as 20 in germanium. Indeed, the variational calculation of McLean and Loudon[20] are rather inaccurate and the perturbation treatment previously used[21] is also inadequate. In order to obtain a quantitative description of the problem one must incorporate the strong anisotropies accurately.

Very recently,[22-24] we have introduced a new method for the analysis of indirect excitons. This approach uses the same formalism as that previously employed for the description of impurity

states in semiconductors.[25,26] The simplicity of the formulation yields a physical interpretation of the various terms present in the Hamiltonian and allows an accurate evaluation of the energies of the exciton levels. In this method one separates the various terms in the exciton Hamiltonian according to their symmetry, thus revealing the importance of the various terms and suggesting simpler models which, while simplifying considerably the analysis, maintain the main features of the problem, thus providing also accurate solutions.

The purpose of the present paper is to describe in detail this method and to give a general investigation of indirect exciton spectra in diamond and zinc-blende crystals. The analogies and similarities with the direct excitons and acceptor impurity states are pointed out and connections with the perturbative approach are discussed. Indeed the indirect-exciton problem represents the bridge between direct excitons and acceptor states. In fact the direct excitons show hydrogenlike spectra while the acceptor impurities have much more complicated spectra. This is understood in terms of the strength of the spherical "spin-orbit" coupling term in the Hamiltonian which is small (~0.2) for direct excitons and large (~0.8) for acceptor impurities. For indirect excitons this term is ~0.4–0.5 and the anisotropy of the conduction electrons introduces a splitting of the fourfold degenerate exciton ground state rendering this coupling larger for the lower state and smaller for the upper state. This produces two series of spectra, one of which is much less hydrogeniclike than the second.

In Sec. II we give the general formulation of the problem. The radial Hamiltonians which describe the exciton states of various symmetries are discussed for the most relevant exciton states. The Hamiltonians are written out explicitly for the ⟨100⟩ and the ⟨111⟩ directions, even though the method can be applied in the case of a general position of the conduction-band minima. The relevance of the various parameters involved in the Hamiltonian are discussed. In Sec. III we classify, using group theory, all relevant exciton states, determine the phonons which assist optical transitions, and discuss the selection rules for transitions in the far-infrared experiments. In Sec. IV the method of solution is presented and comparison with the prediction of the perturbation method is presented. The convergence of the computed eigenvalues is tested and discussed. Extensive comparison with the available experimental data in Ge is shown in Sec. V. We also present results for Si and GaP. The agreement between theory and experiment is good for Si but not for GaP. The difficulties present in the interpretation of GaP are discussed and shown to be consistent with the suggestion that the minimum of the conduction band is not at the X point but very close to it. Finally, in Sec. VI we summarize the main results of the present investigation.

II. FORMULATION OF THE PROBLEM

The band structure of crystals with the diamond and zinc-blende lattice have been studied extensively and are very similar.[11] The valence-band maximum is at $\vec{K}=0$ and is threefold degenerate, neglecting spin. The inclusion of spin and spin-orbit coupling alters the bands by splitting the sixfold-degenerate valence band into an upper fourfold ($J=\frac{3}{2}$) and a lower twofold ($J=\frac{1}{2}$) state separated by a spin-orbit splitting Δ. The absence of inversion symmetry for zinc-blende crystals leads also to the presence of very small linear terms in $\vec{K}$ in the energy versus momentum expression.[27] These terms, which are generally very small and only rarely lead to observable effects, slightly displace the valence-band maximum for $\vec{K}=0$ and will be neglected here. In the effective-mass approximation, the kinetic energy of the hole in the upper band near $\vec{K}=0$ is described by the well-known Kohn-Luttinger Hamiltonian.[28]

$$-H_h(p)=(\gamma_1+\tfrac{5}{2}\gamma_2)\frac{p^2}{2m_0}-\frac{\gamma_2}{m_0}(p_x^2J_x^2+p_y^2J_y^2+p_z^2J_z^2)$$
$$-\frac{2\gamma_3}{m_0}(\{p_xp_y\}\{J_xJ_y\}+\{p_yp_z\}\{J_yJ_z\}$$
$$+\{p_zp_x\}\{J_zJ_x\}), \quad (1)$$

where $\{ab\}=\frac{1}{2}(ab+ba)$, m_0 is the free-electron mass, γ_1, γ_2, and γ_3 are the parameters introduced by Luttinger[29] for the description of the hole dispersion relation near $\vec{K}=0$, $\vec{p}$ is the hole linear momentum operator, and $\vec{J}$ is the angular momentum operator corresponding to spin $\frac{3}{2}$. Hamiltonian (1) is valid in the limit of strong spin-orbit coupling, i.e., when the valence-band spin-orbit splitting Δ at the center of the Brillouin zone is much larger than the exciton binding energy. This is true for most materials except silicon where this contribution is largest because of the small value of Δ in this substance. This effect could be incorporated in our analysis but would make it much more complicated. Therefore, in order to keep the analysis simple, and also since the contribution from the split-off band to the main exciton series can be incorporated by perturbation theory using the same procedure described previously,[21] we will neglect this effect here.

The explicit expression for the electron kinetic operator depends on the position of the conduction-

band minima. Since these minima occur always on high-symmetry direction for which the electron has cylindrical symmetry, we can write

$$H_e = (p_1^2 + p_2^2)/2m_{e\perp} + p_3^2/2m_{e\parallel} , \tag{2}$$

where $m_{e\perp}$ and $m_{e\parallel}$ are the transverse and longitudinal electron masses, respectively. The Hamiltonian (2) is written with respect to the electron ellipsoidal axes 1, 2, and 3 which are, in general, different from the crystal cubic axes x,y, and z used for the hole. Since the operators H_h and H_e must be written in the same coordinate systems, one of the two Hamiltonians must be rotated. Even though the expression for H_e is much simpler than the expression for H_h, it turns out, as we shall see, that it is better to rotate the hole Hamiltonian. The total motion of the electron-hole system is described by the following Hamiltonian

$$H_{ex} = H_e(\vec{p}_e) - H_h(\vec{p}_h) - e^2/(\epsilon_0|\vec{r}_e - \vec{r}_h|) , \tag{3}$$

where ϵ_0 is the static dielectric constant. In writing Hamiltonian (1) we neglect many effects such as electron-hole exchange interaction, wave vector, and frequency dependence of the dielectric constant, which are in general small but could be of some importance in some cases. In the present paper, we also restrict our considerations to states with total crystal momentum equal to $\vec{K}_0$, the difference in $\vec{K}$ space between the valence- and conduction-band extrema. The problem which deals with the investigation of excitons of various K's is treated elsewhere.[30] For the case discussed in the present paper, it is possible to make a transformation to the relative coordinate and replace $\vec{p}_e$ and $\vec{p}_h$ in Eq. (3) with $\vec{p}$.

Using the formalism applied for the case of acceptor impurities which allows us to solve the Hamiltonian for any values of the anisotropies,[25,26] we can rewrite Eq. (3) in a fashion in which the Hamiltonian is separated into parts of different symmetry. We start with the case in which the minima of the conduction band are in the ⟨100⟩ direction. In this case the ellipsoidal axes coincide with the cubic axes and no rotation of the valence- or conduction-band Hamiltonian is required. Equation (3) can be written as

$$H_{ex}(\vec{p}) = \left(\frac{1}{\mu_{0e}} + \gamma_1\right)p^2 - \frac{1}{2\mu_{1e}}\left(\tfrac{2}{3}\right)^{1/2}P_0^{(2)} - \frac{3\gamma_3 + 2\gamma_2}{45m_0}(P^{(2)}\cdot J^{(2)}) + \frac{\gamma_3 - \gamma_2}{18m_0}\left([P^{(2)}\times J^{(2)}]_{-4}^{4} + \frac{\sqrt{70}}{5}[P^{(2)}\times J^{(2)}]_0^4 + [P^{(2)}\times J^{(2)}]_4^4\right) - \frac{e^2}{\epsilon_0 r} \tag{4}$$

with

$$\frac{1}{\mu_{0e}} = \frac{1}{3}\left(\frac{2}{m_{e\perp}} + \frac{1}{m_{e\parallel}}\right) ,$$
$$\frac{1}{\mu_{1e}} = \frac{1}{3}\left(\frac{1}{m_{e\perp}} - \frac{1}{m_{e\parallel}}\right) . \tag{5}$$

In Hamiltonian (4) we have replaced the representation in terms of p and J with a new representation in terms of the irreducible components $P_q^{(2)}$ and $J_q^{(2)}$ of the second-rank Cartesian tensor operators P_{ij} and J_{ij} which are defined in the same manner as in the case of acceptor impurities,[25] i.e.,

$$P_{ik} = 3p_i p_k - \delta_{ik}P^2 ,$$
$$J_{ik} = \tfrac{3}{2}(J_i J_k + J_k J_i) - \delta_{ik}J^2 . \tag{6}$$

The definition of scalar and vector products of irreducible spherical tensor operators is the standard one and has been given previously.[25,31] With the exception of the term proportional to $P_0^{(2)}$, all terms in Eq. (4) appear also in the effective-mass treatment of direct excitons and acceptor impurities and their symmetry and physical meaning were discussed at length elsewhere.[19,25,26] The term in $P_0^{(2)}$, which represents the anisotropy of the conduction-band minima, has a symmetry lower than cubic and is responsible for the splitting of the fourfold-degenerate ground state into a doublet of twofold-degenerate states. The first term in μ_{0e} in Eq. (4) represents the isotropic contribution of the conduction electron. All other terms in p in Eq. (4) describe the valence band. We now use the effective Rydberg

$$R_0 = e^4\mu_0/2\hbar^2\epsilon_0^2 \tag{7a}$$

and the effective Bohr radius

$$a_0 = \hbar^2\epsilon_0/\mu_0 e^2 \tag{7b}$$

as units of energy and length, respectively, as we write Hamiltonian (4) as follows:

$$H_{100} = \frac{1}{\hbar^2}p^2 - \frac{2}{r} - \left(\tfrac{2}{3}\right)^{1/2}\mu_{01}P_0^{(2)} - \frac{1}{9\hbar^2}\mu(P^{(2)}\cdot J^{(2)}) + \frac{1}{9\hbar^2}\delta\left([P^{(2)}\times J^{(2)}]_{-4}^{4} + \frac{\sqrt{70}}{5}[P^{(2)}\times J^{(2)}]_0^4 + [P^{(2)}\times J^{(2)}]_4^4\right) , \tag{8}$$

where

$$1/\mu_0 = 1/\mu_{0e} + \gamma_1 , \tag{9}$$
$$\mu = \tfrac{1}{5}(6\gamma_3 + 4\gamma_2)\mu_0 , \tag{10}$$
$$\delta = (\gamma_3 - \gamma_2)\mu_0 , \tag{11}$$
$$\mu_{01} = \mu_0/\mu_{1e} . \tag{12}$$

The parameters μ and δ have definition which is the same as in the case of direct excitons and acceptors,[17,25] with the difference that quantity $1/\mu_{0e}+\gamma_1$ for indirect excitons must be replaced with $1/m_e+\gamma_1$ for direct excitons and with γ_1 for acceptor impurities. Hamiltonian (8) contains 5 different terms. The first two represent the hydrogen atom. The fourth and the fifth constitute the spherical and cubic "spin-orbit" terms, respectively. The third term, which is present only for the case of indirect excitons, has the lowest symmetry, d-like, and introduces new splittings in the exciton spectrum.

We now consider the case where the minimum of the conduction band is along the $\langle 111\rangle$ direction, such as in germanium. In this case, one must rotate either the hole or the electron part of the Hamiltonian in order to write them in the same reference systems. It would seem that the simplest thing to do would be to write the electron Hamiltonian in the cubic reference system, because the electron Hamiltonian is very simple while the hole Hamiltonian is a 4×4 matrix. Our approach shows, however, that the latter is actually simpler since it has higher symmetry. We, therefore, rewrite the exciton Hamiltonian using the electron ellipsoidal reference system. The valence-band Hamiltonian consists of two parts, one of spherical symmetry and one of cubic symmetry. The first part clearly is not affected. To rotate the cubic part, we see that the operators appearing in the cubic part transform like spherical harmonic Y^4_m,[31] i.e., like the $j=4$ representation of the rotation group. If we denote the Euler angles of the rotation between the $\langle 100\rangle$ and the $\langle 111\rangle$ direction by α, β, and γ [$\alpha=\frac{3}{2}\pi$, $\beta=\cos^{-1}(1/\sqrt{3})$, $\gamma=\frac{3}{4}\pi$] the tensor operator T^4_M is expressed in terms of operators Υ^4_M, quantized along the new z axis, according to

$$T^4_M=\sum_{M'=-4}^{4}\Upsilon^4_{M'}D^4_{M',M}(\alpha,\beta,\gamma)\ , \tag{13}$$

where $D^4_{M',M}$ is the matrix representing the (α,β,γ) rotation in the $j=4$ representation and is given by

$$D^J_{M',M}=e^{i\alpha M'}R^J_{M',M}(\beta)e^{i\gamma M} \tag{14}$$

with

$$R^J_{M',M}(\beta)=\left(\frac{(J+M')!\,(J-M')!}{(J+M)!\,(J-M)!}\right)^{1/2}\times\sum_\sigma\binom{J+M}{J-M'-\sigma}\binom{J-M}{\sigma}\times(-1)^{J-M'-\sigma}\xi^{2\sigma+M'+M}\eta^{2J-2\sigma-M'-M} \tag{15}$$

and

$$\xi=\cos\tfrac{1}{2}\beta;\quad \eta=\sin\tfrac{1}{2}\beta\ . \tag{16}$$

The exciton Hamiltonian for the case for which the conduction-band minimum is in the $\langle 111\rangle$ direction is given by

$$H_{111}=\frac{1}{\hbar^2}p^2-\frac{2}{r}-(\tfrac{2}{3})^{1/2}\mu_{01}P^{(2)}_0-\frac{1}{9\hbar^2}\mu(P^{(2)}\cdot J^{(2)})+\frac{1}{9\hbar^2}\delta\left(\tfrac{4}{3}i[P^{(2)}\times J^{(2)}]^4_{-3}-\tfrac{2}{15}\sqrt{70}[P^{(2)}\times J^{(2)}]^4_0+\tfrac{4}{3}i[P^{(2)}\times J^{(2)}]^4_3\right)\ . \tag{17}$$

Hamiltonian (17) is very similar to expression (8). The only difference lies in the cubic term which has now different operator components and different coefficients. To treat any other case where the conduction-band minima lie in different directions, the only thing to do is to apply the transformation (13) to the cubic term for the appropriate Euler angles.

In order to solve the Schrödinger equations corresponding to the Hamiltonians (8) and (17), we resort to the same method already used for the acceptors. We write the wave function for the exciton states following the L-S coupling scheme used for atomic systems. We use the $\vec{F}$, F_z representation, where $\vec{F}=\vec{L}+\vec{J}$, the sum of angular momentum of the envelope function (L) and of the spin $\frac{3}{2}(J)$ corresponding to the valence-band degeneracy. We write

$$\Psi_{ex}(\vec{r})=\sum_i f_i(r)|L_i,J,F_i,F_{zi}\rangle\ . \tag{18}$$

The expansion in (18), in terms of products of an angular part and of a radial part, is generally infinite. If the cubic and conduction-band anisotropy terms were ignored, F and F_z would be good quantum numbers and the expansion would be finite and very limited. This actually is the case for direct excitons and for acceptor impurities in the "spherical model"[25] approximation. This model is indeed quite good in these cases because the only anisotropy is that of the cubic term and generally μ is much larger than δ.[26] For indirect excitons, in addition to the cubic anisotropy we also have the conduction-band anisotropy and both effects combine to produce a large effect. In Table I the band parameters for indirect materials are given and they are used to calculate the parameters μ, δ, and μ_{01}, which are shown in Table II. In the same table we give, for comparison, the corresponding values of μ and δ for acceptors and for direct excitons. The values of μ and δ for indirect excitons fall in the intermediate region between the small values for direct excitons and the large values for acceptors. The size of the expansion

TABLE I. Band parameters for Ge, Si, GaP, and AlSb. ϵ_0 is the static dielectric constant; m_e^* is the conduction-electron effective mass for direct excitons; $m_{e\parallel}$ and $m_{e\perp}$ are the longitudinal and transversal effective masses, respectively, for indirect excitons; γ_1, γ_2, and γ_3 are the Luttinger valence-band parameters.

Substance	ϵ_0	m_e^*	$m_{e\parallel}$	$m_{e\perp}$	γ_1	γ_2	γ_3
Ge	15.36[a]	0.038[b]	1.588[c]	0.081 52[c]	13.38[d]	4.24	5.69
Si	11.4[a]	•••	0.9163[e]	0.1905[e]	4.22[f]	0.39	1.44
GaP	10.75[g]	0.13[h]	1.7[i]	0.191[i]	4.2[f]	0.98	1.66
AlSb	10.2[g]	0.011[h]	1.5[j]	0.214[j]	4.15[f]	1.01	1.75

[a] R. A. Faulkner, Phys. Rev. 184, 713 (1969).
[b] R. G. Aggarwal, Phys. Rev. B 2, 458 (1970).
[c] B. W. Levinger and D. R. Frankl, J. Phys. Chem. Solids 20, 281 (1961).
[d] E. O. Kane, Phys. Rev. B 11, 3850 (1975).
[e] J. C. Hensel, H. Hasegawa, and M. Nakayama, Phys. Rev. 138, A225 (1965).
[f] P. Lawaetz, Phys. Rev. B 4, 3460 (1971).
[g] M. Hass and B. W. Henvis, J. Phys. Chem. Solids 23, 1099 (1962).
[h] M. Cardona [unpublished results cited in Bowers and Mahan, Phys. Rev. 185, 1073 (1969)].
[i] A. Onton, Phys. Rev. 186, 786 (1969).
[j] R. J. Stirn and W. M. Becker, Phys. Rev. 141, 261 (1966).

must therefore be truncated by successive approximations, i.e., by showing that terms of $L > L_{\max}$ do not appreciably affect the eigensolutions. The functions $|L_i, J, F_i, F_{zi}\rangle$ are eigenfunctions of the total angular momentum in the L-J coupled scheme and the $f_i(r)$ are general radial functions which are defined by the condition that (18) must be an eigenfunction of the Hamiltonians (8) or (17). The $f_i(r)$ satisfy a system of linear differential equations of size $N \times N$, where N is the number of functions involved in the expression (18). The advantage of this approach is that the angular part can be eliminated exactly and analytically from the problem by the use of the "reduced-matrix-element" technique.[31] In the indirect exciton case we have three different type of operators, i.e., $(P^{(2)} \cdot J^{(2)})$, $[P^{(2)} \times J^{(2)}]^4_m$, and $P_0^{(2)}$. Their matrix element with respect to the basis set (18) can be written as

$$\langle L', J, F', F_z' | (P^{(2)} \cdot J^{(2)}) | L, J, F, F_z \rangle = (-1)^{L+J+F} \begin{Bmatrix} F & J & L' \\ 2 & L & J \end{Bmatrix} (J||J^{(2)}||J)(L'||P^{(2)}||L)\delta_{F',F}\delta_{F_z',F_z} , \tag{19}$$

$$\langle L', J, F', F_z' | [P^{(2)} \times J^{(2)}]^4_m | L, J, F, F_z \rangle$$

$$= 3(-1)^{F'-F_z'}[(2F'+1)(2F+1)]^{1/2} \begin{pmatrix} F & 4 & F \\ -F_z' & & F_z \end{pmatrix} \begin{pmatrix} J' & J & 0 \\ L' & L & 2 \\ F' & F & 2 \end{pmatrix} (L'||P^{(2)}||L)(J||J^{(2)}||J) , \tag{20}$$

TABLE II. The parameters μ, δ, and μ_{01} are calculated using the band parameters given in Table I. The direct exciton, indirect exciton, and acceptor cases are considered. Equations (10)–(12) are used for indirect excitons. For direct excitons and acceptors the corresponding expressions for μ and δ are obtained using the procedure given in the text and μ_{01} is zero.

	Direct excitons		Indirect excitons			Acceptors	
Substance	μ	δ	μ	δ	μ_{01}	μ	δ
Ge	0.257	0.037	0.469	0.067	0.178	0.764	0.108
Si	•••	•••	0.252	0.130	0.171	0.483	0.249
GaP	0.233	0.057	0.352	0.086	0.196	0.661	0.162
AlSb	0.031	0.008	0.388	0.099	0.178	0.701	0.178

$$\langle L',J,F',F_z'|P_0^{(2)}|L,J,F,F_z\rangle = (-1)^{F'-F_z'-L'+J+F}[(2F'+1)(2F+1)]^{1/2} \begin{pmatrix} F' & 2 & F \\ -F_z & 0 & F_z \end{pmatrix} \begin{Bmatrix} L' & F' & J \\ F & L & 2 \end{Bmatrix} (L'||P^{(2)}||L)\delta_{F_z',F_z} . \quad (21)$$

These matrix elements are expressed in terms of the 3-j, 6-j, and 9-j symbols[32] and the reduced matrix elements $(J||J^{(2)}||J)$ and $(L''||P^{(2)}||L)$ which have been reported previously.[25,26] The radial part is contained in the reduced matrix elements $(L'||P^{(2)}||L)$ and the rest of the terms are just numbers. Since parity is a good quantum number, i.e., $\Delta L = L' - L = 0, \pm 2$, we will have different sets of differential equation systems for even (s like) and odd (p like) states. Here we denote by "s" and "p" states which are mostly composed of $L=0$ or $L=1$ states, respectively. For s states ($L=0$) we have two possible series of states $S_{\pm 1/2}^{3/2}$ and $S_{\pm 3/2}^{3/2}$, where the upper index refers to the quantum number F and the lower to F_z, again meaning those of the state that contributes most to the eigenfunction expansion. Since all eigenstates are Kramer doublets, we will drop from now on the $\pm$ sign for F_z in the definition of the states. For p states ($L=1$) we can have six possible series states, i.e., $P_{1/2}^{1/2}$, $P_{1/2}^{3/2}$, $P_{1/2}^{5/2}$, $P_{3/2}^{3/2}$, $P_{3/2}^{5/2}$, $P_{5/2}^{5/2}$. The connection between this notation in terms of approximate rotation-group symmetry and the exact crystal symmetry is discussed in Sec. III. The basis functions entering in the expression for each state are easily determined and they are given in Table III, for the case of ⟨100⟩ direction and in Table IV for the ⟨111⟩ direction, including terms up to $L=4$ for even states and $L=5$ for odd states. Before closing this section we want to describe an approximation to Hamiltonians (8) and (17) which define the "axial model."[22-24] It consists in assuming that the valence band is axially symmetric about the longitudinal direction of the conduction-band ellipsoid, i.e., neglecting its anisotropy in the plane perpendicular to the ellipsoid axis. This is accomplished by dropping the term $m \neq 0$ in the cubic term, thus giving

$$H = \frac{1}{\hbar^2}p^2 - \frac{2}{r} - (\tfrac{2}{3})^{1/2}\mu_{01}P_0^{(2)} - \frac{1}{9\hbar^2}\mu(P^{(2)}\cdot J^{(2)}) + \frac{1}{9\hbar^2}\alpha\delta(\sqrt{70}/5)[P^{(2)}\times J^{(2)}]_0^4 , \quad (22)$$

where for ⟨100⟩ direction

$$\alpha = 1 \quad (23a)$$

and for ⟨111⟩ direction

$$\alpha = -\tfrac{2}{3} . \quad (23b)$$

The conceptual and mathematical advantage of the axial model are considerable, in that they simplify greatly the level of the analysis, thus allowing the treatment of more complicated problems.[30] This is easily seen considering the number of basis states involved in the expression (18). We have seen that for s states and including angular momenta up to $L=4$, we have, from Table II and III, 15 terms for both the $S_{3/2}^{3/2}$ and $S_{1/2}^{3/2}$ in the ⟨100⟩ direction and 20 terms for both states in the ⟨111⟩ direction. Using the axial model the number of terms is reduced to 9 for the $S_{1/2}^{3/2}$ and to 8 for the $S_{3/2}^{3/2}$ in both directions. For p-like states the reduction is given more drastic, in fact, in the ⟨100⟩ direction the $F_z = \pm\frac{1}{2}$ is reduced from 21 to 11 terms, while the $F_z = \pm\frac{3}{2}, \pm\frac{5}{2}$ states are reduced

TABLE III. Basis functions entering in the expansion of indirect exciton wave functions for ⟨100⟩ direction conduction-band minima. The notation $|L,J,F,F_z\rangle$ is explained in the text. The quantity J is omitted here because it is the same ($J=\frac{3}{2}$) for all functions. For even (odd) states all terms up to $L_{max}=4$ ($L_{max}=5$) are included.

Even L states						Odd L states					
L	F	F_z	L	F	F_z	L	F	F_z	L	F	F_z
0	$\frac{3}{2}$	$\frac{1}{2}$	0	$\frac{3}{2}$	$\frac{3}{2}$	1	$\frac{1}{2}$	$\frac{1}{2}$	1	$\frac{3}{2}$	$\frac{3}{2}$
2	$\frac{1}{2}$	$\frac{1}{2}$	2	$\frac{3}{2}$	$\frac{3}{2}$	1	$\frac{3}{2}$	$\frac{1}{2}$	1	$\frac{5}{2}$	$\frac{3}{2}$
2	$\frac{3}{2}$	$\frac{1}{2}$	2	$\frac{5}{2}$	$\frac{3}{2}$	1	$\frac{5}{2}$	$\frac{1}{2}$	1	$\frac{5}{2}$	$-\frac{5}{2}$
2	$\frac{5}{2}$	$\frac{1}{2}$	2	$\frac{7}{2}$	$\frac{3}{2}$	3	$\frac{3}{2}$	$\frac{1}{2}$	3	$\frac{1}{2}$	$\frac{3}{2}$
2	$\frac{7}{2}$	$\frac{1}{2}$	2	$\frac{5}{2}$	$-\frac{5}{2}$	3	$\frac{5}{2}$	$\frac{1}{2}$	3	$\frac{5}{2}$	$\frac{3}{2}$
2	$\frac{7}{2}$	$-\frac{7}{2}$	2	$\frac{7}{2}$	$-\frac{5}{2}$	3	$\frac{7}{2}$	$\frac{1}{2}$	3	$\frac{7}{2}$	$\frac{3}{2}$
4	$\frac{5}{2}$	$\frac{1}{2}$	4	$\frac{5}{2}$	$\frac{3}{2}$	3	$\frac{9}{2}$	$\frac{1}{2}$	3	$\frac{9}{2}$	$\frac{3}{2}$
4	$\frac{7}{2}$	$\frac{1}{2}$	4	$\frac{7}{2}$	$\frac{3}{2}$	3	$\frac{7}{2}$	$-\frac{7}{2}$	3	$\frac{5}{2}$	$-\frac{5}{2}$
4	$\frac{9}{2}$	$\frac{1}{2}$	4	$\frac{9}{2}$	$\frac{3}{2}$	3	$\frac{9}{2}$	$-\frac{7}{2}$	3	$\frac{7}{2}$	$-\frac{5}{2}$
4	$\frac{11}{2}$	$\frac{1}{2}$	4	$\frac{11}{2}$	$\frac{3}{2}$	3	$\frac{9}{2}$	$\frac{9}{2}$	3	$\frac{9}{2}$	$-\frac{5}{2}$
4	$\frac{7}{2}$	$-\frac{7}{2}$	4	$\frac{5}{2}$	$-\frac{5}{2}$	5	$\frac{7}{2}$	$\frac{1}{2}$	5	$\frac{7}{2}$	$\frac{3}{2}$
4	$\frac{9}{2}$	$-\frac{7}{2}$	4	$\frac{7}{2}$	$-\frac{5}{2}$	5	$\frac{9}{2}$	$\frac{1}{2}$	5	$\frac{9}{2}$	$\frac{3}{2}$
4	$\frac{9}{2}$	$\frac{9}{2}$	4	$\frac{9}{2}$	$-\frac{5}{2}$	5	$\frac{11}{2}$	$\frac{1}{2}$	5	$\frac{11}{2}$	$\frac{3}{2}$
4	$\frac{11}{2}$	$-\frac{7}{2}$	4	$\frac{11}{2}$	$-\frac{5}{2}$	5	$\frac{13}{2}$	$\frac{1}{2}$	5	$\frac{13}{2}$	$\frac{3}{2}$
4	$\frac{11}{2}$	$\frac{9}{2}$	4	$\frac{11}{2}$	$\frac{11}{2}$	5	$\frac{7}{2}$	$-\frac{7}{2}$	5	$\frac{7}{2}$	$-\frac{5}{2}$
						5	$\frac{9}{2}$	$-\frac{7}{2}$	5	$\frac{9}{2}$	$-\frac{5}{2}$
						5	$\frac{9}{2}$	$\frac{9}{2}$	5	$\frac{11}{2}$	$-\frac{5}{2}$
						5	$\frac{11}{2}$	$-\frac{7}{2}$	5	$\frac{11}{2}$	$\frac{11}{2}$
						5	$\frac{11}{2}$	$\frac{9}{2}$	5	$\frac{13}{2}$	$-\frac{13}{2}$
						5	$\frac{13}{2}$	$-\frac{7}{2}$	5	$\frac{13}{2}$	$-\frac{5}{2}$
						5	$\frac{13}{2}$	$\frac{9}{2}$	5	$\frac{13}{2}$	$\frac{11}{2}$

from 21 to two systems of order 10 and 8, respectively. In the ⟨111⟩ direction the number of basis functions is reduced, in the axial model, to the same number of states as in the ⟨100⟩ direction from the original number of 28 for both the $F_z=\pm\frac{1}{2},\pm\frac{5}{2}$ and the $F_z=\pm\frac{3}{2}$ states. Within the axial model, one has the same number of basis states for any direction of the conduction-band minima, since that same Hamiltonian applies with the proper factor α for any given direction. The advantages of the axial model are therefore evident. The validity of this model depends on the relative strength of cubic anisotropy δ with respect to the strength of the electron anisotropy parameter μ_{ie} and of the spherical term μ. Its validity depends also, as we shall see in Sec. IV, on the direction of the conduction-band minima. In practice we will see that the axial model provides an excellent description of the indirect exciton states.

TABLE IV. Basis functions entering in the expansion of indirect exciton wave functions for ⟨111⟩ direction conduction-band minima. All quantities are the same as those defined in Table III.

Even L states						Odd L states					
L	F	F_z	L	F	F_z	L	F	F_z	L	F	F_z
0	$\frac{3}{2}$	$\frac{1}{2}$	0	$\frac{3}{2}$	$\frac{3}{2}$	1	$\frac{1}{2}$	$\frac{1}{2}$	1	$\frac{3}{2}$	$\frac{3}{2}$
2	$\frac{1}{2}$	$\frac{1}{2}$	0	$\frac{3}{2}$	$-\frac{3}{2}$	1	$\frac{3}{2}$	$\frac{1}{2}$	1	$\frac{5}{2}$	$\frac{3}{2}$
2	$\frac{3}{2}$	$\frac{1}{2}$	2	$\frac{3}{2}$	$\frac{3}{2}$	1	$\frac{5}{2}$	$\frac{1}{2}$	1	$\frac{3}{2}$	$-\frac{3}{2}$
2	$\frac{5}{2}$	$\frac{1}{2}$	2	$\frac{5}{2}$	$\frac{3}{2}$	1	$\frac{5}{2}$	$-\frac{5}{2}$	1	$\frac{5}{2}$	$-\frac{3}{2}$
2	$\frac{7}{2}$	$\frac{1}{2}$	2	$\frac{7}{2}$	$\frac{3}{2}$	3	$\frac{3}{2}$	$\frac{1}{2}$	3	$\frac{3}{2}$	$\frac{3}{2}$
2	$\frac{5}{2}$	$-\frac{5}{2}$	2	$\frac{3}{2}$	$-\frac{3}{2}$	3	$\frac{5}{2}$	$\frac{1}{2}$	3	$\frac{5}{2}$	$\frac{3}{2}$
2	$\frac{7}{2}$	$-\frac{5}{2}$	2	$\frac{5}{2}$	$-\frac{3}{2}$	3	$\frac{7}{2}$	$\frac{1}{2}$	3	$\frac{7}{2}$	$\frac{3}{2}$
2	$\frac{7}{2}$	$\frac{7}{2}$	2	$\frac{7}{2}$	$-\frac{3}{2}$	3	$\frac{9}{2}$	$\frac{1}{2}$	3	$\frac{9}{2}$	$\frac{3}{2}$
4	$\frac{5}{2}$	$\frac{1}{2}$	4	$\frac{5}{2}$	$\frac{3}{2}$	3	$\frac{5}{2}$	$-\frac{5}{2}$	3	$\frac{3}{2}$	$-\frac{3}{2}$
4	$\frac{7}{2}$	$\frac{1}{2}$	4	$\frac{7}{2}$	$\frac{3}{2}$	3	$\frac{7}{2}$	$-\frac{5}{2}$	3	$\frac{5}{2}$	$-\frac{3}{2}$
4	$\frac{9}{2}$	$\frac{1}{2}$	4	$\frac{9}{2}$	$\frac{3}{2}$	3	$\frac{7}{2}$	$\frac{7}{2}$	3	$\frac{7}{2}$	$-\frac{3}{2}$
4	$\frac{11}{2}$	$\frac{1}{2}$	4	$\frac{11}{2}$	$\frac{3}{2}$	3	$\frac{9}{2}$	$-\frac{5}{2}$	3	$\frac{9}{2}$	$-\frac{9}{2}$
4	$\frac{5}{2}$	$-\frac{5}{2}$	4	$\frac{5}{2}$	$-\frac{3}{2}$	3	$\frac{9}{2}$	$\frac{7}{2}$	3	$\frac{9}{2}$	$-\frac{3}{2}$
4	$\frac{7}{2}$	$-\frac{5}{2}$	4	$\frac{7}{2}$	$-\frac{3}{2}$	5	$\frac{7}{2}$	$\frac{1}{2}$	3	$\frac{9}{2}$	$\frac{9}{2}$
4	$\frac{7}{2}$	$\frac{7}{2}$	4	$\frac{9}{2}$	$-\frac{9}{2}$	5	$\frac{9}{2}$	$\frac{1}{2}$	5	$\frac{7}{2}$	$\frac{3}{2}$
4	$\frac{9}{2}$	$-\frac{5}{2}$	4	$\frac{9}{2}$	$-\frac{3}{2}$	5	$\frac{11}{2}$	$\frac{1}{2}$	5	$\frac{9}{2}$	$\frac{3}{2}$
4	$\frac{9}{2}$	$\frac{7}{2}$	4	$\frac{9}{2}$	$\frac{9}{2}$	5	$\frac{13}{2}$	$\frac{1}{2}$	5	$\frac{11}{2}$	$\frac{3}{2}$
4	$\frac{11}{2}$	$-\frac{11}{2}$	4	$\frac{11}{2}$	$-\frac{9}{2}$	5	$\frac{7}{2}$	$-\frac{5}{2}$	5	$\frac{13}{2}$	$\frac{3}{2}$
4	$\frac{11}{2}$	$-\frac{5}{2}$	4	$\frac{11}{2}$	$-\frac{3}{2}$	5	$\frac{7}{2}$	$\frac{7}{2}$	5	$\frac{7}{2}$	$-\frac{3}{2}$
4	$\frac{11}{2}$	$\frac{7}{2}$	4	$\frac{11}{2}$	$\frac{9}{2}$	5	$\frac{9}{2}$	$-\frac{5}{2}$	5	$\frac{9}{2}$	$-\frac{9}{2}$
						5	$\frac{9}{2}$	$\frac{7}{2}$	5	$\frac{9}{2}$	$-\frac{3}{2}$
						5	$\frac{11}{2}$	$-\frac{11}{2}$	5	$\frac{9}{2}$	$\frac{9}{2}$
						5	$\frac{11}{2}$	$-\frac{5}{2}$	5	$\frac{11}{2}$	$-\frac{9}{2}$
						5	$\frac{11}{2}$	$\frac{7}{2}$	5	$\frac{11}{2}$	$-\frac{3}{2}$
						5	$\frac{13}{2}$	$-\frac{11}{2}$	5	$\frac{11}{2}$	$+\frac{9}{2}$
						5	$\frac{13}{2}$	$-\frac{5}{2}$	5	$\frac{13}{2}$	$-\frac{9}{2}$
						5	$\frac{13}{5}$	$\frac{7}{2}$	5	$\frac{13}{2}$	$-\frac{3}{2}$
						5	$\frac{13}{2}$	$\frac{13}{2}$	5	$\frac{13}{2}$	$\frac{9}{2}$

III. GROUP-THEORETICAL ANALYSIS

Before discussing the solution of the problem formulated in the previous section, it is useful to classify, using group theory, all relevant exciton states and to show the connection between crystal symmetry and rotation-group symmetry.

The exciton wave function can be written as[33]

$$\psi(\vec{r}_e,\vec{r}_h)=\sum_i \chi_{ex}^{(i)}(\vec{r}_e-\vec{r}_h)\phi_h^{(i)}(\vec{r}_h)\phi_e(\vec{r}_e)\ , \qquad (24)$$

where ϕ_e and ϕ_h are the Bloch functions for the electron and the hole, $\chi^{(i)}$ is the envelope function which describes the relative electron-hole motion, and i runs over the degenerate valence-band states. The symmetry of the exciton wave function is determined by the direct product of the representations for the envelope, hole, and electron functions. We first consider the diamond crystal case.[34] In this case, the point group is O_h and the symmetry of the valence band at $\vec{K}=0$ is Γ_8^+. The conduction-band minimum is Δ_1 for silicon and L_1 for germanium. Since in the present analysis the exchange between electron and the hole is neglected, we will use the single group rotation for the conduction band. For s-like states, the envelope function can be dropped from the direct product while, for p-like states, the envelope function has Γ_{15} symmetry for the point group O_h. For indirect excitons the symmetry group of the electron is a subgroup of that of the hole, so that the symmetry group for the exciton is just the electron symmetry group itself. The results of the symmetry analysis are given in Table V and VI for the ⟨100⟩ and the ⟨111⟩ cases, respectively. Since the representations L_4^+ and L_5^+ are degenerate because of time reversal we see that, apart from accidental degeneracy, the exciton states always split into twofold-degenerate levels. The symmetry analysis for the III-V compounds, whose point group is T_d, is easily obtained.

Optical transitions, from the crystal ground state to the exciton states, must be assisted by phonons in order to conserve the total crystal momentum. The analysis for the determination of which phonons assist optical transitions has been discussed previously[21] and one sees that phonons of any symmetry can assist transitions to both s-like exciton

TABLE V. Crystal symmetry classification for indirect exciton states in Ge. In the first column the atomic symmetry is reported; in the second column the symmetry for the corresponding states in the direct exciton and acceptor cases is shown; in the third column the crystal symmetry for indirect excitons is given; in the last column the correspondence between crystal symmetry and the $|L,J,F,F_z\rangle$ representation is given.

Atomic species	Direct excitons and acceptors	Indirect excitons	Correspondence with $\|L,F,F_z\rangle$ representation
s like	Γ_8^+	$L_4^+ + L_5^+$	$\|0,\frac{3}{2},\frac{3}{2}\rangle$
		L_6^+	$\|0,\frac{3}{2},\frac{1}{2}\rangle$
p like	$2\Gamma_8^-$	$4L_6^-$	$\|1,\frac{1}{2},\frac{1}{2}\rangle,\|1,\frac{3}{2},\frac{1}{2}\rangle$
	$+\Gamma_7^-$		$\|1,\frac{5}{2},\frac{1}{2}\rangle,\|1,\frac{5}{2},-\frac{5}{2}\rangle$
	$+\Gamma_6^-$	$+2(L_4^- + L_5^-)$	$\|1,\frac{3}{2},\frac{3}{2}\rangle,\|1,\frac{5}{2},\frac{3}{2}\rangle$

states for III-V compounds and Si, while for Ge only TO(L_3') and LA(L_2') phonons are allowed.

In the far-infrared experiments, transitions between the exciton ground state and excited exciton states are observed. The dipole operator Γ_{15} develops, in the indirect exciton symmetry group, into $L_1 + L_3$ for the $\langle 111\rangle$ direction case and into $\Delta_1 + \Delta_5$ for the $\langle 100\rangle$ direction case. As a result all transitions between the s like and the p like are allowed.

IV. METHOD OF SOLUTION

Before discussing the method employed for the solution of the radial equations for the various exciton states, we will present the solution of these equations in the perturbative limit, that is, in the limit in which μ, δ, and μ_{01} can be treated as small effects. Even though we have previously seen[22] that this is not the case in practice, this procedure is still quite useful because it gives insight into the problem and provides simple analytical solutions for the energies of the most important exciton states. These analytical expressions are not quantitatively accurate, for the comparison with experimental data; however, they represent a useful single qualitative tool for the assignment of the various states.

For s-like exciton states we have previously carried out the perturbative analysis.[21] However, it is useful to treat it here because the present approach is quite different and provides new insight and helps the understanding of the axial model.

In the perturbative limit, the s-like states can couple only with d-like states. For the $\langle 100\rangle$ direction we write

$$E_{1s}(\Delta_6) = 1 + \sum_{i=1}^{6}\sum_{n=1}^{\infty} \frac{|\langle 0,\frac{3}{2},\frac{1}{2};f_{1s}(r)|H_{100}|f_{nd}(r);2,F_i,F_{zi}\rangle|^2}{1-E_n} \quad , \tag{25}$$

where the $f_{nl}(r)$ represent the radial functions for the hydrogen atom. The $\sum_{n=1}^{\infty}$ actually means summation for discrete states and integration over continuum states. The matrix elements in (25) are performed exactly and using expressions (19)–(21). After straightforward calculations one gets

$$E_{1s}^{100}(\Delta_6) = 1 + [\mu^2 + \tfrac{24}{25}\delta^2 + \tfrac{4}{5}\mu_{01}^2 - \tfrac{4}{5}\mu_{01}(\mu - \tfrac{6}{5}\delta)]\,4S_1(0) \tag{26}$$

when $S_1(0)$ is the same as defined previously.[18] Analogous procedure for the Δ_7 state shows that we can write

$$E_{1s}^{100} = 1 + [\mu^2 + \tfrac{24}{25}\delta^2 + \tfrac{4}{5}\mu_{01}^2 \pm \tfrac{4}{5}\mu_{01}(\mu - \tfrac{6}{5}\delta)]\,4S_1(0) \ , \tag{27}$$

where the (+) sign applies to the Δ_7 states and the (−) sign to the Δ_6 states. If we restrict ourselves to the axial model, the summation in expression (25) for i contains now 5 terms for the $F_z = \pm\frac{1}{2}$ state and 4 terms for the $F_z = \pm\frac{3}{2}$ state, and we obtain

$$E_{1s}^{100,\,\text{axial}} = 1 + [\mu^2 + \tfrac{14}{25}\delta^2 + \tfrac{4}{5}\mu_{01}^2 \pm \tfrac{4}{5}\mu_{01}(\mu - \tfrac{6}{5}\delta)]\,4S_1(0) \ . \tag{28}$$

By comparing expression (28) with expression (27) we see that, within the perturbation limit, the axial model approximation does not alter the splitting between the anistropy split ground-state components and affect only the term in δ^2. From Table

TABLE VI. Crystal symmetry classification for indirect exciton state in silicon. All quantities are the same as those defined in Table V.

Atomic species	Direct excitons and acceptors	Indirect excitons	Correspondence with $\|L,F,F_z\rangle$ representation
s like	Γ_8^+	Δ_6	$\|0,\frac{3}{2},\frac{1}{2}\rangle$
		Δ_7	$\|0,\frac{3}{2},\frac{3}{2}\rangle$
p like	$2\Gamma_8^-$	$3\Delta_6$	$\|1,\frac{1}{2},\frac{1}{2}\rangle,\|1,\frac{3}{2},\frac{1}{2}\rangle$
	$+\Gamma_7^-$		$\|1,\frac{5}{2},\frac{1}{2}\rangle$
	$+\Gamma_6^-$	$3\Delta_7$	$\|1,\frac{3}{2},\frac{3}{2}\rangle,\|1,\frac{5}{2},\frac{3}{2}\rangle$
			$\|1,\frac{5}{2},-\frac{5}{2}\rangle$

II we see that δ is always smaller than μ so that the contribution of the "nonaxial terms" ($\frac{2}{5}\delta^2$) is always quite small.

For the $\langle 111\rangle$ direction the analysis proceeds in a very similar manner and one gets

$$E_{1s}^{111} = 1 + [\mu^2 + \tfrac{24}{25}\delta^2 + \tfrac{4}{5}\mu_{01}^2 \pm \tfrac{4}{5}\mu_{01}(\mu + \tfrac{4}{5}\delta)]\,4S_1(0), \tag{29}$$

and, using the axial model,

$$E_{1s}^{111,\,\mathrm{axial}} = 1 + [\mu^2 + \tfrac{56}{225}\delta^2 + \tfrac{4}{5}\mu_{01}^2 \pm \tfrac{4}{5}\mu_{01}(\mu + \tfrac{4}{5}\delta)]\,4S_1(0)\ . \tag{30}$$

By comparing expressions (29) and (30) with expressions (27) and (28) we see that there is a simple relationship between the results obtained in the $\langle 100\rangle$ and the $\langle 111\rangle$ direction. In fact the only difference between the two directions consist in changing δ into $-\frac{2}{3}\delta$ in going from the $\langle 100\rangle$ to the $\langle 111\rangle$ direction in the term linear in μ_{1e}. This result is valid for any direction of the conduction-band minima, that is, once the answer is known for say the $\langle 100\rangle$ direction, a simple factor substitution which is related to the rotation from the given direction to a different one gives the solution for the case of the conduction-band minima lying in this direction.

To obtain the energy expression for the $2s$-like states, the only change is with respect to the $1s$ states in the radial integrals and one gets

$$E_{2s} = \tfrac{1}{4} + \tfrac{1}{2}[\mu^2 + \alpha^2\tfrac{14}{25}\delta^2 + \tfrac{2}{25}(12 - 7\alpha^2)\delta^2 + \tfrac{4}{5}\mu_{01}^2 \pm \tfrac{4}{5}\mu_{01}(\mu - \tfrac{6}{5}\alpha\delta)]S_2(0) \tag{31}$$

with α given by Eq. (23) and $S_2(0)$ is the same quantity as defined previously.[18] In expression (31) we have separated the axial contribution ($\frac{14}{25}\alpha^2\delta^2$) from the total contribution in the cubic anisotropy.

For p-like indirect exciton states, the perturbative expressions are derived here for the first time. If we include only first-order perturbation theory, the energies of the p-like exciton states are obtained, for the $\langle 100\rangle$ case, by solving a 3×3 determinant for the Δ_6 and another 3×3 for the Δ_7 states. For the $\langle 111\rangle$ direction case, one obtains a 2×2 determinant for $L_4^- + L_5^-$ states and a 4×4 for the L_6^- states. It is possible to write the solutions of these determinants in a very simple form if one neglects small coupling terms between different F states. In the $\langle 100\rangle$ direction we have, for Δ_6 symmetry

$$E_1 = -\tfrac{1}{4}\mu\ , \tag{32a}$$

$$E_2 = \tfrac{1}{5}(\mu - \tfrac{2}{5}\mu_{01})\ , \tag{32b}$$

$$E_3 = \tfrac{1}{20}(-\mu + \tfrac{12}{5}\delta + \tfrac{8}{5}\mu_{01})\ , \tag{32c}$$

and for Δ_7 symmetry

$$E_4 = \tfrac{1}{5}(\mu + \tfrac{2}{5}\mu_{01})\ , \tag{32d}$$

$$E_5 = \tfrac{1}{20}\{-\mu - \tfrac{1}{5}[6\delta + 4\mu_{01} + (324\delta^2 + 36\mu_{01}^2 - 144\,\delta\mu_{01})^{1/2}]\}, \tag{32e}$$

$$E_6 = \tfrac{1}{20}\{-\mu - \tfrac{1}{5}[6\delta + 4\mu_{01} - (324\delta^2 + 36\mu_{01}^2 - 144\delta\mu_{01})^{1/2}]\}\ . \tag{32f}$$

In the $\langle 111\rangle$ direction, we write, for $L_4^- + L_5^-$,

$$E_1 = \tfrac{1}{5}(\mu + \tfrac{2}{5}\mu_{01}) \tag{33a}$$

$$E_2 = \tfrac{1}{20}(-\mu + \tfrac{12}{5}\delta + \tfrac{2}{5}\mu_{01}) \tag{33b}$$

and for L_6^- symmetry,

$$E_3 = -\tfrac{1}{4}\mu\ , \tag{33c}$$

$$E_4 = \tfrac{1}{5}(\mu - \tfrac{2}{5}\mu_{01})\ , \tag{33d}$$

$$E_5 = \tfrac{1}{20}\{-\mu - \tfrac{1}{5}[6\delta + \mu_{01} + (324\delta^2 + 81\mu_{01}^2 - 36\delta\mu_{01})^{1/2}]\}\ , \tag{33e}$$

$$E_6 = \tfrac{1}{20}\{-\mu - \tfrac{1}{5}[6\delta + \mu_{01} - (324\delta^2 + 81\mu_{01} - 36\delta\mu_{01})^{1/2}]\}\ . \tag{33f}$$

The perturbation analysis presented here is not accurate because the values of μ, δ, and μ_{1e} for indirect excitons are large. In Fig. 1, we show the behavior of the lowest states as a function of

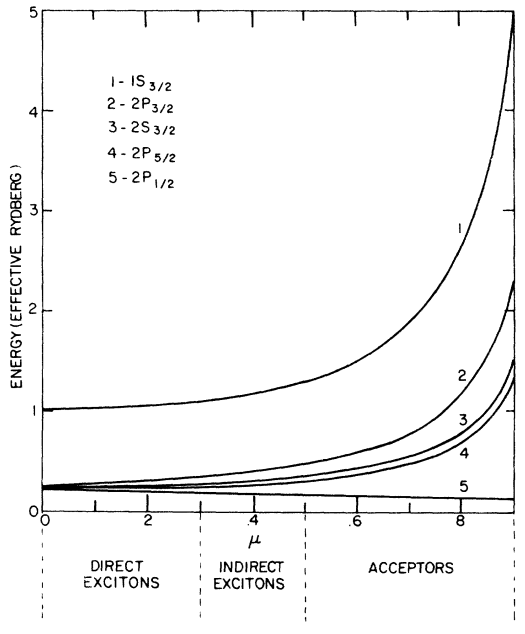

FIG. 1. Energy levels for the most important exciton and acceptor states using the "spherical" model (Ref. 25) as a function of the parameter μ [Eq. (10)].

the quantity μ.[25] From Table II we have seen that μ for indirect excitons is typically around 0.4 and for this value of μ the solutions are outside the validity of the perturbation approved. In addition δ and μ_{01} contribute to rendering the solution even less perturbative. Expressions (26)–(33) therefore provide only a very rough description of the indirect exciton states and a more accurate method of solution is required.

We now discuss the method of solution for the system of radial differential equations presented in Sec. II for the various states. Since an exact solution of the problem is clearly impossible, we solve these equations by the same method as that previously used for acceptor states. In the present case, however, we assume that the trial wave functions are linear combinations of exponential functions times the lowest polynomials which correctly behaves at the origin for the lowest L value.

For even L (s-like) states we write

$$f_i(r) = \sum_{m=1}^{N_i} c_{i,m} e^{-\alpha_{i,m} r} \tag{34}$$

and, for odd L (p-like) states,

$$f_i(r) = r \sum_{m=1}^{N_i} d_{i,m} e^{-\alpha_{i,m} r} \ . \tag{35}$$

While the linear parameters $c_{i,m}$ and $d_{i,m}$ are used as variational parameters in order to minimize the energy, the other quantities, i.e., N_i and $\alpha_{i,m}$, are fixed. The number of terms in the expressions (34) and (35) is determined using the convergence criterion, that is, by checking that a large set does not affect the eigenvalues within a required accuracy. In addition we allow this quantity N_i, to be dependent on the angular momentum L, that is, N_i decreases as L increases because the higher L the weaker the contribution of the state to the eigenfunction expansion. The parameters $\alpha_{i,m}$ are chosen in geometrical progression and their range of values is wide enough to cover all actual situations met in studying the indirect exciton spectrum.

In Table VII we present the results for all relevant exciton states in germanium using the values of μ, δ, and μ_0 given in Table II and the basis functions shown in Table IV. In the same table we also give the results obtained using the axial model (22). The comparison between the two calculations is, indeed, very good for all the states and supports the validity of the axial model. As discussed in Sec. II, the number of basis states involved in the expansion (18) is considerably reduced when the axial model is employed. This reduction allows us to check the convergence of the reported eigenvalues. In Table VIII we report the dependence of the eigenvalues upon the values of

TABLE VII. Indirect exciton energy levels for Ge. The parameters shown in Tables I and II are used for their calculations. Comparison with the axial model is also shown. All results are obtained using the basis states given in Table IV. The lowest 3 states for even L and the lowest 5 states for odd L are reported. The energy unit is meV.

Even L			
L_6^+	Axial model	$L_4^+ + L_5^+$	Axial model
3.183	3.168	4.206	4.185
0.883	0.877	1.329	1.322
0.584	0.564	0.748	0.744
Odd L			
L_6^-	Axial model	$L_4^- + L_5^-$	Axial model
1.136	1.128	1.915	1.903
0.879	0.831	0.938	0.933
0.774	0.812	0.790	0.789
0.541	0.537	0.540	0.538
0.461	0.458	0.399	0.396

$L_{\max}$. The number of basis functions increases only by 4 when going from any L value to the next highest, and we see that all eigenvalues show good convergence for $L_{\max} \geq 4$. Appreciable differences are, however, seen when going from $L_{\max}=2$ to $L_{\max}=4$, and therefore all the calculations presented in this paper are performed using $L_{\max}=4$ and have a convergence of better than 0.1 meV. A similar study for odd L states shows that calculations using $L_{\max}=5$ have also comparable accuracy. In Tables IX, X, and XI the results for Si, GaP, and AlSb are shown using the number of basis states given in Table III and the parameters shown in Table II.

In Fig. 2, we show the s-like components for the lowest $L_4^+ + L_5^+$ and L_6^+ states in Ge. For comparison we also show the hydrogenic solution, valid in the

TABLE VIII. Convergence of the most important even L exciton states in germanium and silicon using the axial model. Five different values of $L_{\max}$ were used in the calculations.

State \ $L_{\max}$	0	2	4	6	8
Germanium					
$L_4^+ + L_5^+$	2.649	3.922	4.185	4.238	4.253
L_6^+	2.649	3.130	3.168	3.173	3.174
Silicon					
Δ_7	12.951	14.514	14.584	14.585	14.586
Δ_6	12.951	14.059	14.123	14.124	14.125

TABLE IX. Indirect exciton energy levels for Si. The parameters shown in Tables I and II are used for these calculations. Comparison with the axial model is also shown. All results are obtained using the basis states given in Table VII. The lowest 3 levels for even L and the lowest 5 levels for odd L are reported. The energy unit is meV.

Even L			
Δ_6	Axial model	Δ_7	Axial model
14.199	14.123	14.658	14.584
3.752	3.728	3.934	3.913
2.058	2.041	2.069	2.014
Odd L			
Δ_6	Axial model	Δ_7	Axial model
4.582	4.562	4.949	4.923
3.548	3.540	3.483	3.332
2.638	2.623	2.908	3.021
2.095	2.086	2.256	2.245
1.643	1.637	1.637	1.584

perturbative region. It is, indeed, evident the large deviation of the two states, especially the $L_4^+ + L_5^+$, from the hydrogenic behavior and necessity of the present treatment which is valid for any value of μ, δ, and μ_{01}. A quantity of special interest is the value of the function at the origin. For the hydrogenic case, we would have $|\psi_{1s}(0)|^2 = 4$, while from Fig. 2 we see that $|\psi_{1s}^{L_4^+ + L_5^+}(0)|^2 = 18.92$ and $|\psi_{1s}^{L_6^+}(0)|^2 = 7.36$, which are considerably different. In addition the wave functions for the two indirect exciton states are considerably more localized than the hydrogenic wave function. In Fig. 3 the wave functions for the analogous states

TABLE X. Indirect exciton energy levels for GaP. All quantities are the same as those defined in Table VIII.

Even L			
X_6	Axial model	X_7	Axial model
16.995	16.950	18.954	18.912
4.612	4.598	5.396	5.386
2.699	2.688	2.878	2.866
Odd L			
X_6	Axial model	X_7	Axial model
5.774	5.761	7.194	7.182
4.371	4.366	4.203	4.096
2.816	2.809	3.692	3.771
2.694	2.688	3.315	3.312
2.065	2.061	2.084	2.058

TABLE XI. Indirect exciton energy levels for AlSb. All quantities are the same as those defined in Table VIII.

Even L states			
X_6	Axial model	X_7	Axial model
20.431	20.355	22.729	22.658
5.604	5.579	6.485	6.467
3.322	3.304	3.461	3.456
Odd L states			
X_6	Axial model	X_7	Axial model
7.088	7.067	8.685	8.662
5.304	5.294	5.123	4.971
3.307	3.297	4.404	4.509
3.215	3.203	3.984	3.977
2.530	2.523	2.548	2.509

in silicon are shown, and we see that their deviation from the hydrogenic solution is considerably smaller than for Ge due to the fact that μ for silicon is much smaller than its corresponding value in Ge and that, for ⟨100⟩ direction minima, the splitting between Δ_6 and Δ_7 is smaller, as easily seen from the perturbative expressions, than the corresponding splittings in the ⟨111⟩ direction.

Before closing this section, we show in Figs. 4, 5, and 6 the behavior of the lowest indirect exciton states for the case of ⟨100⟩ conduction-band minima as a function of the parameters μ, δ, and μ_{01}. These figures are useful in determining the effect of the uncertainty of any of the three parameters on the calculated indirect exciton spectrum. Since it would be quite difficult to show the combined effect of the three parameters, we show the effect of each individual one. These figures, to-

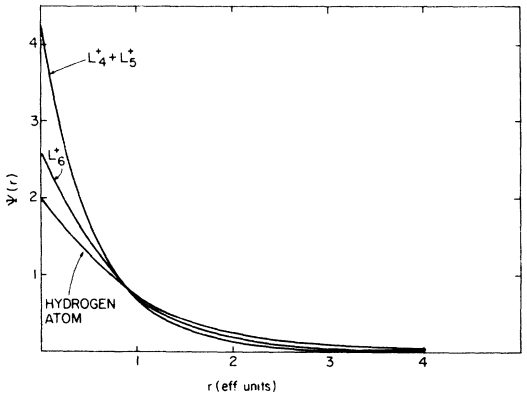

FIG. 2. s-like components of the ground-state doublet in Ge. The hydrogen 1s radial wave function is also shown for comparison.

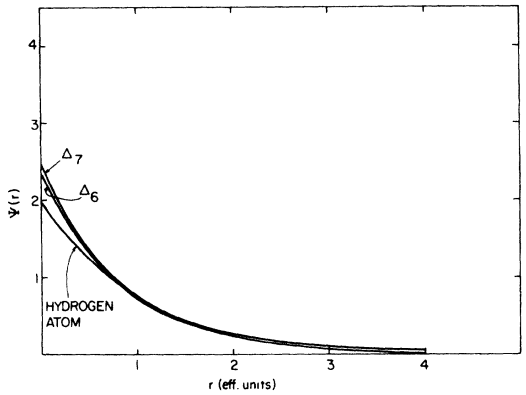

FIG. 3. s-like components of the ground-state doublet in Si. The hydrogen 1s radial wave function is also shown for comparison.

gether with the perturbative expressions, should be very useful in estimating the effect of variations in the valence-band parameters on the excitonic spectrum in those materials where the band parameters are not known accurately.

V. COMPARISON WITH EXPERIMENT

The only materials for which experimental data are available are Ge, Si, and GaP. In Table XII we compare the calculated and the observed binding energies for these materials. As previously

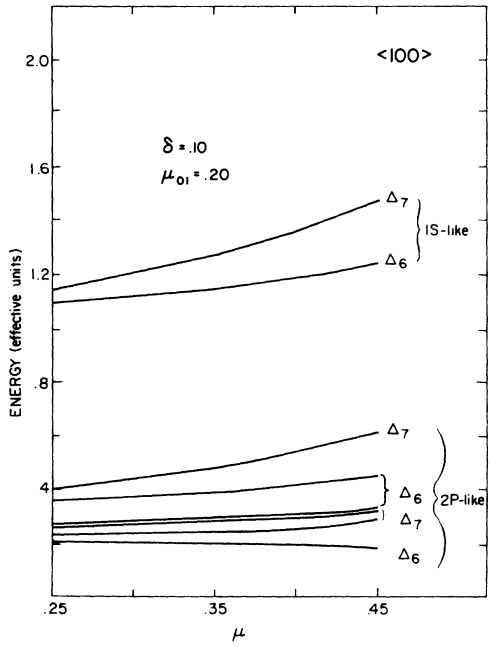

FIG. 4. Energy levels of the most important indirect exciton states as a function of the parameter μ.

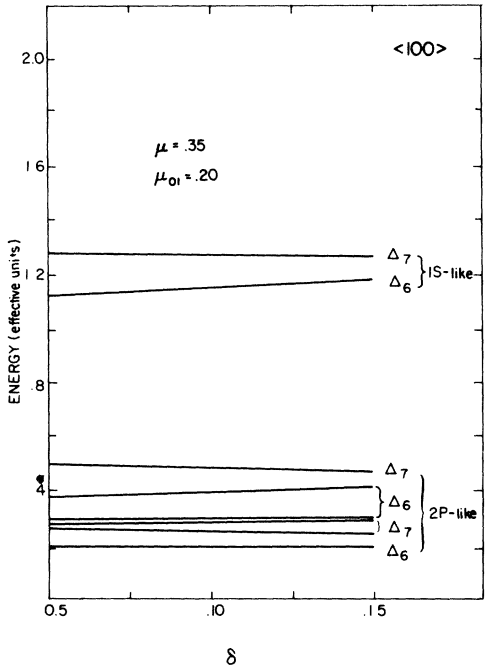

FIG. 5. Energy levels of the most important indirect exciton states as a function of the parameter δ.

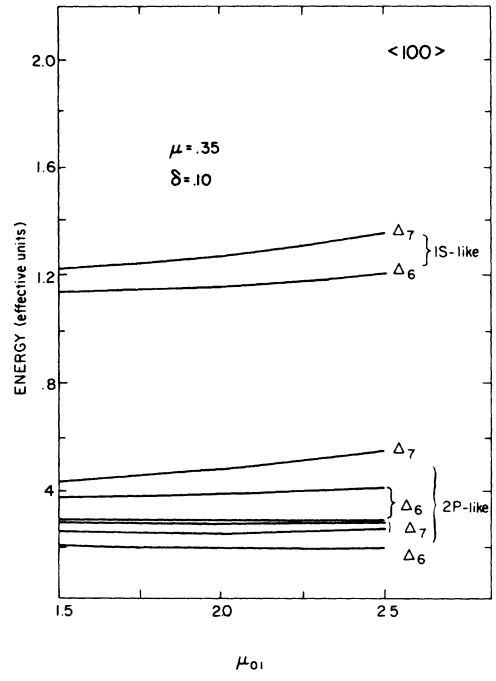

FIG. 6. Energy levels of the most important indirect exciton states as a function of the parameter μ_{01}.

TABLE XII. Indirect exciton binding energies in group IV elements and III–V compounds. The energy unit is meV. The last column gives the reference for the experimental data.

Crystal	Symmetry	$E_b(1s)$	Experiment	References
Ge	L_6^+	3.18	3.14	3
	$L_4^+ + L_5^+$	4.21	4.15	3
Si	Δ_6	14.12	14.7	36
	Δ_7	14.66		
GaP	X_6	16.99	13.8	a
	X_7	18.95		
AlSb	X_6	20.43		
	X_7	22.73		

[a]R. A. Street and W. Senske, Phys. Rev. Lett. 37, 1292 (1976).

discussed,[22,23] excellent agreement is obtained for Ge both in the absolute value and in the splitting of the anisotropy split ground-state components. In Table XIII we show the transitions observed in recent far-infrared absorption spectra by Buchanan and Timusk[10] and by Gershenzon *et al.*[6-9] together with the calculated transitions. The correspondence between theory and experiment is quite good, both in energy and in their temperature dependence. All the peaks which are seen at low temperature are associated with transitions from the lower exciton state ($1S_{3/2}^{3/2}$) while the lines with rapid temperature dependence are associated with transition from the upper exciton state ($1S_{1/2}^{3/2}$). The new line at 1.3, present in the experimental data of Buchanan and Timusk,[10] is much lower than what one would expect from an hydrogenic model (at 2.0 meV) and is a direct evidence of the importance of conduction-band anisotropy in the exciton spectra of germanium. The extra fine structure present in the data of Gershenzon *et al.*[6-9] is well accounted for by transition to high excited states.

In silicon, the agreement for binding energies is also good and can be improved by including the effect of the splitoff band. This effect, which is largest in silicon because of its small spin-orbit splittings, is calculated by perturbation theory[21] to be 0.4 meV. This brings the calculated values to 14.5 and 15.0 for the heavy and light exciton, respectively. Excellent agreement is also found for the 1*s*-2*s* separation with the data of Shaklee and Nahory.

In comparing the splitting of the ground-state doublet with the experimental information available, the situation is not as straightforward as in Ge, where this quantity is directly measured in modulated absorption experiments. In Si, no splitting is visible in absorption,[35] but analysis of the temperature dependence of the ratio of LO to TO assisted luminescence intensity[36] indicates a value of the splitting between 0.3 and 0.5 meV, in agreement with our calculated value, 0.46 meV. The

TABLE XIII. Comparison between theory and the experimental data of Buchanan and Timusk (Ref. 10 in text). The theoretical assignment of the transitions is given in the last column using the notation nL_{Fz}^{F} and only the basis states which appreciably contribute to any given level are shown.

Experiment		Theory	
Energy (meV)	Type	Energy (meV)	Assigned transitions
1.3	Temp. dep.	1.27	$1S_{1/2}^{3/2} \rightarrow 2P_{3/2}^{3/2}$
2.1	Temp. dep.	2.05	$1S_{1/2}^{3/2} \rightarrow 2P_{1/2}^{3/2}$
2.35		2.29, 2.30	$1S_{3/2}^{3/2} \rightarrow 2P_{3/2}^{3/2}$; $1S_{1/2}^{3/2} \rightarrow (2P_{1/2}^{5/2}, 2P_{-5/2}^{5/2})$
2.44	Temp. dep.	2.40, 2.41	$1S_{1/2}^{3/2} \rightarrow 2P_{3/2}^{5/2}$; $1S_{1/2}^{3/2} \rightarrow (2P_{1/2}^{5/2}, 2P_{-5/2}^{5/2})$
2.87	Temp. dep.		Higher excited states and continuum of heavy exciton series
3.00	Temp. dep.		
3.13		3.07	$1S_{3/2}^{3/2} \rightarrow 2P_{1/2}^{3/2}$
3.35		3.33	$1S_{3/2}^{3/2} \rightarrow (2P_{1/2}^{5/2}, 2P_{-5/2}^{5/2})$
3.42		3.42, 3.43	$1S_{3/2}^{3/2} \rightarrow 2P_{3/2}^{5/2}$; $1S_{3/2}^{3/2} \rightarrow (2P_{1/2}^{5/2}, 2P_{-5/2}^{5/2})$

reason why the splitting is not observed in aborption may be that the oscillator strength of one of the two states is much smaller than the other,[35] perhaps because of destructive interference between processes with phonon scattering in the valence or in the conduction band. Other explanations, such as the influence of the exchange interaction on energies and selection rules, seem to be in quantitative disagreement with the data.[37] Finally, we consider the GaP case. The agreement between theory and experiment is poor. In fact, the theory predicts binding energies of 17.8 and 19.6 meV for the ground-state doublet while the data suggests a much smaller value. The disagreement is outside the kind of error expected for the theory and suggests that, provided the experimental value for the binding energy is correct, we have an inadequate description of the conduction-band structure. Indeed it has been recently pointed out that the construction band minimum in GaP is not at the zone edge but somewhat close to it.[38] This would imply a "camel back" type of $E(K)$ rather than parabolic. Preliminary results[39] show that indeed better agreement is obtained. Lastly, no experimental data for AlSb are available.

VI. CONCLUSIONS

In the present paper we have described a new approach to the effective-mass theory of indirect excitons in semiconductors. In this method, similar to that used for acceptor impurities, one separates the various terms in the Hamiltonian according to their symmetry. In addition to the valence-band anisotropy one has a strong electron anistropy term which makes the perturbation analysis inaccurate. Using rotation-group techniques to separate the angular and the radial parts, accurate solutions are obtained for the most important exciton states. A simple, but equally accurate model, the "axial model," is described. The validity of this model, which depends on the relative strength of the electron and the hole anisotropy, is generally satisfied and allows a considerable simplification of the analysis. The importance of this model is more fully appreciated when other effects are taken into account in the exciton Hamiltonian such as inclusion of energy-momentum dispersion,[40] external fields, etc. Finally, extensive comparison with experimental data show the validity of the present method.

---

*Present address: T. J. Watson IBM Research Center, P. O. Box 218, Yorktown Heights, N.Y. 10598.

†Supported by NSF through Grant No. DMR-76-01058.

[1]E. J. Johnson, in *Semiconductors and Semimetals*, edited by K. Willardson and A. Beer (New York, 1967), Vol. 3, p. 153.

[2]For a review, see, e.g., *Excitons at High Densities*, edited by H. Haken and S. Nikitine, *Springer Tracts in Modern Physics*, Vol. 73 (Springer-Verlag, Berlin, 1975).

[3]A. Frova, G. A. Thomas, R. E. Miller, and E. O. Kane, Phys. Rev. Lett. 34, 1592 (1975); T. Nishino, M. Takeda, and Y. Hamakawa, Solid State Commun. 12, 1137 (1973).

[4]G. G. MacFarlane, T. P. McLean, J. E. Quarrington, and V. Roberts, Phys. Rev. 108, 1377 (1957); *ibid.* 111, 1245 (1958); J. Phys. Chem. Solids 8, 388 (1959); Proc. Phys. Soc. 71, 863 (1958); S. Zwerdling, L. M. Roth, and B. Lax, Phys. Rev. 109, 2207 (1958); J. Phys. Chem. Solids 8, 397 (1959).

[5]See, for example, Ref. 1.

[6]E. M. Gershenzon, G. N. Gol'tsman, and N. G. Ptitsina, Pis'ma Zh. Eksp. Teor. Fiz. 16, 228 (1972) [JETP Lett. 16, 161 (1972)].

[7]E. M. Gershenzon, G. N. Gol'tsman and N. G. Ptitsina, Pis'ma Zh. Eksp. Teor. Fiz. 18, 160 (1973) [JETP Lett. 18, 93 (1973)].

[8]V. S. Vasilov, N. V. Guzeev, V. A. Zayats, V. L. Kononenko, T. S. Mandel'stam, and V. N. Murzin, Pis'ma Zh. Eksp. Teor. Fiz. 17, 480 (1973) [JETP Lett. 17, 345 (1973)].

[9]V. N. Kononenko, T. S. Mandel'stam, V. N. Murzin, V. S. Vasilov, and V. A. Zayats, Proceedings of the XII International Conference on the Physics of Semiconductors, Stuttgart, 1974, p. 152 (unpublished).

[10]M. Buchanan and T. Timusk, Proceedings of the XIII International Conference on the Physics of Semiconductors, 1976 (unpublished).

[11]See, for example, M. L. Cohen and T. K. Bergstresser, Phys. Rev. 141, 789 (1966).

[12]F. Herman, Phys. Rev. 95, 847 (1954).

[13]W. P. Dumke, Phys. Rev. 118, 938 (1960).

[14]M. R. Lorenz, R. Chicotka, G. D. Pettit, and P. J. Dean, Solid State Commun. 8, 693 (1970).

[15]K. M. Ghanekar and R. J. Sladek, Phys. Rev. 146, 505 (1966); R. J. Stirn and W. M. Becker, Phys. Rev. 141, 621 (1966).

[16]S. A. Abgyan, A. V. Lishina, and V. K. Subashiev, Fiz. Tverd. Tela 6, 2852 (1964) [Sov. Phys. Solid State 6, 2266 (1965)]; J. P. Walter and M. L. Cohen, Phys. Rev. 183, 763 (1969).

[17]A. Baldereschi and N. O. Lipari, Phys. Rev. Lett. 25, 373 (1970).

[18]A. Baldereschi and N. O. Lipari, Phys. Rev. B 3, 439 (1971).

[19]N. O. Lipari, Nuovo Cimento B 23, 51 (1974).

[20]T. P. McLean and R. Loudon, J. Phys. Chem. Solids 13, 1 (1960).

[21]N. O. Lipari and A. Baldereschi, Phys. Rev. B 3, 2497 (1971).

[22]N. O. Lipari and M. Altarelli, Solid State Commun. 18, 951 (1976).

[23]M. Altarelli and N. O. Lipari, Phys. Rev. Lett. 36, 619 (1976).

[24]M. Altarelli and N. O. Lipari, Proceedings of the XIII International Conference on the Physics of Semiconductors, Rome, 1976 (unpublished).
[25]A. Baldereschi and N. O. Lipari, Phys. Rev. B 8, 2693 (1973).
[26]A. Baldereschi and N. O. Lipari, Phys. Rev. B 9, 1525 (1974).
[27]G. Dresselhaus, Phys. Rev. 100, 580 (1955); E. O. Kane, J. Phys. Chem. Solids 1, 249 (1957).
[28]J. M. Luttinger and W. Kohn, Phys. Rev. 97, 869 (1955).
[29]J. M. Luttinger, Phys. Rev. 102, 1030 (1956).
[30]See Ref. 23; also M. Altarelli and N. O. Lipari (unpublished).
[31]A. R. Edmonds, *Angular Momentum in Quantum Mechanics* (Princeton U.P., Princeton, N.J., 1960).
[32]M. Rotenberg, R. Bivins, N. Metropolis, and J. K. Wooten, *The 3-j and 6-j Symbols* (Technology, Cambridge, Mass., 1959); we have also written a computer routine which calculates the 3-*j*, 6-*j*, and 9-*j* coefficients.
[33]See, for example, the review by R. S. Knox, in *Solid State Physics*, edited by F. Seitz and D. Turnbull (Academic, New York, 1965), Suppl. 50.
[34]Throughout this paper, the notation is that used by G. F. Koster, in *Solid State Physics*, edited by F. Seitz and D. Turnbull (Academic, New York, 1957), Vol. 5.
[35]M. Capizzi, F. Evangelisti, and A. Frova, in Proceedings of the XIII International Conference on the Physics of Semiconductors, Rome, 1976 (unpublished). M. Capizzi, A. Frova, F. Evangelisti, and P. Valfrê, Solid State Commun. (to be published).
[36]D. L. Smith, R. B. Hammond, M. Chen, S. A. Lyon, and T. C. McGill, in Proceedings of the XIII International Conference on the Physics of Semiconductors Rome, 1976 (unpublished).
[37]E. O. Kane (private communication).
[38]P. J. Dean and D. C. Herbert, J. Lumines. 14, 55 (1976).
[39]M. Altarelli and N. O. Lipari (unpublished).
[40]M. Altarelli and N. O. Lipari (unpublished).